

1 **Physical Drivers of the November 2023 Heatwave in Rio de**
2 **Janeiro**

3 Catherine C. Ivanovich¹, Adam H. Sobel^{1,2,3}, Radley M. Horton^{2,4}, Ana M. B. Nunes⁵, Rosmeri
4 Porfirio da Rocha⁶, and Suzana J. Camargo^{2,4}

5
6 ¹Department of Earth and Environmental Sciences, Columbia University, New York, NY, United States

7 ²Lamont-Doherty Earth Observatory, Columbia University, Palisades, NY, United States

8 ³Department of Applied Physics and Applied Mathematics, Columbia University, New York, NY, United States

9 ⁴Columbia Climate School, Columbia University, New York, NY, United States

10 ⁵Instituto de Geociências, Universidade Federal do Rio de Janeiro, Rio de Janeiro, RJ, Brazil

11 ⁶Instituto de Astronomia, Geofísica e Ciências Atmosféricas, Universidade de São Paulo, São Paulo, SP, Brazil

12

13

14 *Correspondence to:* Catherine Ivanovich (cci2107@columbia.edu)

15 **Abstract**

16 As extreme heat has not historically been a major hazard for the city of Rio de Janeiro, the
17 November 2023 Heatwave magnitude and timing were staggering. Here we conduct a case study
18 of reanalysis data and high-resolution projections to explore the event drivers and characterize
19 the evolving extreme heat risk in the city of Rio de Janeiro. We find that the heatwave was
20 associated with atmospheric blocking, potentially linked to the 2023-24 El Niño event. Soil
21 moisture declines increased surface sensible heat flux, and elevated sea surface temperatures
22 reduced coastal cooling. The heatwave was preceded by weeks of suppressed precipitation and
23 terminated by the onset of rain. We also find a significant historical increase in the frequency of
24 high heat days throughout Brazil and a lengthening of the heat season in the city of Rio de
25 Janeiro. The frequency of the city’s austral spring heat extremes is expected to increase further in
26 the future, highly dependent upon our future emissions pathway. These results emphasize the
27 rapidly emerging risk for extreme heat in the city of Rio de Janeiro.

28
29 **1 Introduction**

30 In the spring of 2023, the city of Rio de Janeiro experienced a high impact heatwave that
31 caught the world’s attention. Media sources ranging from local reporting to international news
32 companies centered stories on the event’s record-breaking temperature magnitudes and
33 unseasonal timing, arriving earlier in the warm season than typical heatwaves (Correio
34 Braziliense, 2023; Hughs and Jeanet, 2023). The impacts of the extreme heat were widely
35 publicized in part due to the tragic death of a concertgoer hospitalized during a Taylor Swift
36 performance in Rio de Janeiro on November 17, with news articles reporting heat-induced
37 cardiovascular distress as the cause of death (Nguyen, 2023). Sources also report that the stadium
38 in which the concert took place experienced higher temperatures than those measured in the open
39 air, as well as a lack of cooling equipment and insufficient water for attendees (Nguyen, 2023;
40 Jornal Nacional, 2023). Such complexities highlight that extreme heat experienced by
41 individuals on the ground can far exceed temperatures measured at local weather stations,
42 depending on infrastructure and the capacity for cooling interventions (Wilby et al., 2021; Nahlik
43 et al., 2017). However, the meteorological event itself is of course one of the preconditions for
44 societal impacts. We therefore explore the physical mechanisms behind the heatwave as one key
45 step towards improving preparation for the impact of future extreme heat events.

46 Throughout Brazil, the highest temperatures occur climatologically in low latitude and
47 low altitude regions in the interior of the country, such as the cities of Teresina (Piauí, in the
48 Northeast region of Brazil) and Palmas (Tocantins, in the Central-West region of Brazil; Alvares
49 et al., 2013), both of which are far from Rio de Janeiro. Extreme temperatures tend to be
50 intensified by land-atmosphere interactions, as dry soils partition more energy into sensible heat
51 (Geirinhas et al., 2018). These relationships between the atmosphere and land surface processes
52 increase the likelihood of compound extreme heat and drought events and intensify impacts on
53 agriculture (Cirino et al., 2015), worker productivity for outdoor laborers (Bitencourt et al.,
54 2021), wildfire risk (Libonati et al., 2022), and direct impacts on human health (Zhao et al.,
55 2019). As the frequency and intensity of extreme heat throughout Brazil has increased
56 significantly in the past decades and is projected to continue in the future (Feron et al., 2019;
57 Regoto et al., 2021; Bitencourt et al., 2020), the widespread socio-economic impacts of these
58 events are likely to grow.

59 While Rio de Janeiro is the second most populous city in Brazil (Instituto Brasileiro de
60 Geografia e Estatística 2022) and the third most populous city in South America (United Nations
61 Department of Economic and Social Affairs Population Division 2022), few studies have
62 focused on extreme heat in the city. On one hand, Rio de Janeiro has not historically been a
63 major hotspot of extreme heat in Brazil and has experienced fewer heatwaves relative to other
64 major cities in the country (Geirinhas et al., 2018). Further, the numerous microclimates within
65 the city, influenced by its coastal setting and complex topography, complicate the study of local
66 heatwave dynamics. Indeed, there is large spatial variability in temperature extremes across the
67 Rio de Janeiro metropolitan area compared to other Brazilian cities (Alvares et al., 2013).
68 However, impactful heatwaves in recent decades have increasingly drawn attention from public
69 health officials and scientific communities alike. Recent literature has explored the dynamics and
70 mortality impacts of extreme temperatures during heatwaves in 2010 (Geirinhas et al., 2019) and
71 2013/2014 (Geirinhas et al., 2022) and has begun to investigate compound heatwave and drought
72 events throughout Southeast Brazil (Geirinhas et al., 2021). There is also building evidence that
73 temperature extremes are increasing in intensity and frequency throughout Brazil, including the
74 city of Rio de Janeiro (Regoto et al., 2021; Bitencourt et al., 2019). Climate variability also plays
75 an important role in modulating temperatures over this area, including large scale modes of
76 climate variability such as the El Niño-Southern Oscillation (Rehbein and Ambrizzi 2023; Cai et

77 al., 2020; Shimizu and Ambrizzi 2015), the Pacific Decadal Oscillation, and the Atlantic
78 Multidecadal Oscillation (He et al., 2021). Should more intense, frequent, and unseasonably
79 early extreme heat events take place in the future in the city of Rio de Janeiro, these heatwaves
80 may have increased impacts on human health due to potential exceedance of unprecedented
81 temperature thresholds and individuals' lack of preparation for these events. In a tropical city
82 where baseline temperatures are already relatively high, small shifts in the temperature
83 distribution can have large impacts on the frequency of extremes (Cheng et al., 2019),
84 particularly at thresholds relevant to human health outcomes (Vecellio et al., 2022). These health
85 risks are compounded by the humidity in Rio de Janeiro, a coastal city with ample moisture
86 sources from the ocean and surrounding vegetation, priming the region for humid heat extremes
87 which are physiologically more dangerous to human health than dry heat (Mora et al., 2017).

88 In this study, we explore the meteorological conditions that led to the extreme heat event
89 in November 2023 in the city of Rio de Janeiro. We identify drivers of the exceptional
90 magnitude and persistence of the extreme temperatures, as well as their early arrival in the
91 calendar year. We compare these conditions to those associated with typical heatwaves in the
92 region, and particularly events taking place in the spring season. We then consider how extreme
93 spring temperature events have shifted throughout the historical period, and how we might
94 expect them to change in the future with ongoing anthropogenic climate change.

95

96 **2 Methods**

97 **2.1 Data**

98 This analysis employs both station-based observations and reanalysis data. Initial
99 analyses are conducted on subdaily station data from the city of Rio de Janeiro, accessed via the
100 Met Office Hadley Center's HadISD station-based dataset (Dunn 2019) and the Rio Alert
101 System produced by the Rio de Janeiro City Hall (Sistema Alerta Rio da Prefeitura do Rio de
102 Janeiro 2024). Three airport weather stations are available from HadISD for the city of Rio de
103 Janeiro, namely the Galeão/Antonio Carlos Jobim International Airport (located on the island
104 Ilha do Governador within the Guanabara Bay), the Campo Délio Jardim De Mattos Airport (an
105 Air Force base located in the city's North Zone), and the Santos Dumont Airport (a waterfront
106 airport located near the city center). Six additional stations from the Rio Alert System dataset
107 record measurements from the tops of various community and commercial buildings, including

108 hotels, schools, and warehouses. These stations are located in distinct areas of the city, whose
109 topographical and coastal complexities contribute to various microclimates. These stations thus
110 record distinct values, both instantaneously and on average (see Fig. S1), a challenge that has
111 been previously identified in the literature (Lyra et al., 2018; Dereczynski et al., 2013). We
112 therefore base the majority of our analysis on reanalysis data and compare the identified patterns
113 with station data when possible. This comparison is particularly important for extreme events, as
114 the magnitude of extreme heat has been shown to be biased in reanalysis products due to their
115 spatial and temporal smoothing of observations (Rogers et al., 2021; Raymond et al., 2020).
116 Further, the human experience of heat stress is inherently hyperlocal, meaning that the distinct
117 microclimates existing throughout the city can control heat stress exposure and the efficiency of
118 adaptation strategies. However, the present study is primarily concerned with the regional drivers
119 of the extreme event rather than its absolute magnitude. Reanalysis provides continuous spatial
120 coverage and a wide array of internally consistent meteorological variables, which warrants its
121 use for the application here.

122 Hourly meteorological data are retrieved from the fifth major global reanalysis of the
123 European Centre for Medium-Range Weather Forecasts (ERA5), including 2-meter temperature,
124 2-meter dewpoint temperature, volumetric soil water for layer 1 (0-7 cm, where the surface is at
125 0 cm), surface pressure, geopotential height at 500 hPa and 200 hPa, precipitation, evaporation,
126 2-meter horizontal winds, and vertical velocity at 500 hPa (Hersbach et al., 2020). From this
127 hourly data, daily maximum temperature, daily total precipitation, and daily means of all other
128 variables are calculated from 1979-2023. Daily mean sea surface temperature (SST) data from
129 1979-2023 is also retrieved from the NOAA 1/4° Daily Optimum Interpolation Sea Surface
130 Temperature (OISST) dataset (Huang et al., 2021).

131 We also explore the future evolution of temperature extremes over the city of Rio de
132 Janeiro using the NEXGDDP dataset (Thrasher et al., 2022). This data product is statistically
133 downscaled from the Coupled Model Intercomparison Project Phase 6 (CMIP6) models, with a
134 spatial resolution of 0.25 degrees and outputs variables on a daily temporal scale. We directly
135 retrieve daily maximum temperature data through the end of the century under the Shared
136 Socioeconomic Pathways (SSPs) SSP2-4.5 and SSP5-8.5 for the 23 models which output this
137 variable and pair of scenarios for each day in the calendar year through 2100.

138 Because of Rio de Janeiro’s complex coastal and mountainous terrain, projections may
139 not accurately capture fine scale differences in the city’s climate. For example, recent literature
140 has shown that the coastal cooling relative to inland areas experienced in regions such as the
141 eastern United States may be underestimated by global climate models (Raymond and Mankin
142 2019). These biases are greatest in regions with large land-ocean surface temperature contrasts,
143 however, and Rio de Janeiro’s location in the tropics, as well as the fact that the extreme events
144 analyzed in this study take place in the spring when this temperature gradient should be
145 relatively small, may mute these biases compared to other regions and seasons. In order to
146 address these potential sources of error, we generate a set of synthetic time series based on
147 NEXGDDP projections which retain the seasonality and variability recorded in the historical
148 reanalysis data from ERA5. We use a percentile matching technique in which we first bin all
149 data for the grid cell which includes the city of Rio de Janeiro during a historical base period
150 (1981-2013) into one-percentile bins for both the NEXGDDP and ERA5 datasets. We
151 additionally bin all NEXGDDP data from this grid cell into one-percentile bins during one
152 midcentury period (2041-2060) and one end-of-century period (2081-2100). We then calculate
153 the temperature delta for each percentile bin between the base period and both the midcentury
154 and the end-of-century periods in the NEXGDDP data. Finally, we add these percentile-specific
155 change factors to every data point in each associated bin in the historical ERA5 base period.

156

157 **2.2 Methodology**

158 We first create time series for the historical day-of-year climatologies of variables in the
159 city of Rio de Janeiro and compare them to the evolution throughout 2023. All anomalies are
160 calculated relative to historical mean calendar date values (i.e., the daily maximum temperature
161 anomaly on November 18, 2023 is calculated by subtracting the mean daily maximum
162 temperatures on November 18 in all previous years in the historical record from the recorded
163 absolute magnitude of the event). We also generate maps of concurrent meteorological variables
164 relevant to the extreme heat event for the greater region outside of Rio de Janeiro. We compare
165 these spatial patterns to those experienced during previous extreme heat events in Rio de Janeiro,
166 calculated as 99th percentile daily maximum temperature days across all seasons for the grid cell
167 which includes the Galeão International Airport weather station. We then select for events that
168 occur in the September-November (SON) austral spring season.

169 We also quantify how extreme heat in the city of Rio de Janeiro is shifting using a variety
170 of methods. We first calculate the trend in the frequency of extreme temperatures over the
171 historical record in Brazil, defining these extreme temperatures using both absolute and relative
172 thresholds. We select these thresholds as 30°C and the locally defined 90th percentile daily
173 maximum temperature at each grid cell. These thresholds are chosen in order to investigate
174 impactful temperature magnitudes while ensuring sufficient sample size for the trend analysis.

175 We also visualize the broadening of the extreme heat season, calculated based on the
176 number of days between the start of the first heatwave and end of the last heatwave of the
177 season. A heatwave is defined here as a three-day period with consecutive daily maximum
178 temperatures above the 50th percentile of daily maximum temperatures across the two hottest
179 months of the year in the city of Rio de Janeiro (January and February); this 50th percentile
180 threshold is equal to about 31.4°C. This heat season definition is informed by a definition used
181 by the United States Environmental Protection Agency (US EPA 2021), adapted to better reflect
182 Rio de Janeiro's lower temporal variability in temperature due to its tropical location.

183 Finally, we calculate how spring temperature distributions have already changed in Rio
184 de Janeiro by comparing early and late historical periods in ERA5 for the grid cell which
185 includes the Galeão International Airport weather station. Distributions are calculated from
186 annual spring maximum temperatures in the city of Rio de Janeiro and fit using GEV
187 distributions, which have been shown to well capture extreme temperature distributions (Powis
188 et al., 2023; Van Oldenborgh et al., 2022). For comparison, we also plot GEV distributions for
189 early and late historical periods in the NEXGDDP model data before applying our bias-
190 correction technique. The location parameter and spread of the model data distributions during
191 these periods is much lower than that of ERA5 (Fig. S2), further motivating our use of synthetic
192 time series to explore how these distributions may change in the future.

193 We then use the bias-corrected NEXGDDP data for the 23 models which report daily
194 maximum temperature for each day in the calendar year under the aforementioned SSP2-4.5 and
195 SSP5-8.5 scenarios during a midcentury and end-of-century time period. We additionally
196 evaluate the impact of only using models which most accurately reproduce the historical
197 observed daily maximum temperature record in the city of Rio de Janeiro. We calculate the
198 Perkins skill score to evaluate the similarity between probability density functions of daily
199 maximum temperature in the reanalysis dataset (ERA5) and each of the 23 global climate models

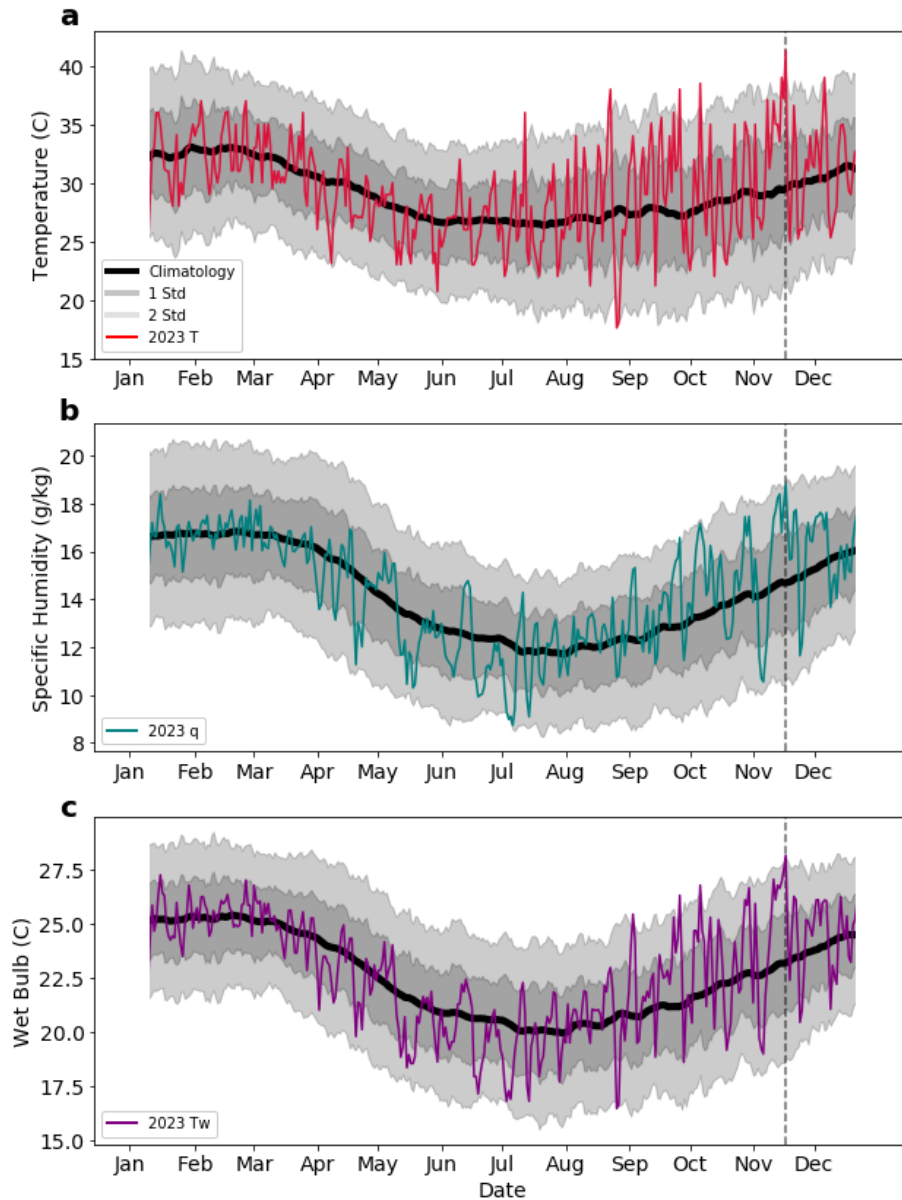
200 during the historical period. These skill scores are calculated as the cumulative minimum
201 between the observed and modeled distributions of each binned value (Perkins et al., 2007). We
202 finally select the 6 climate models which exhibit skill scores greater than 0.8, indicating that
203 these models capture over 80% of the observed probability density functions. The result of this
204 analysis is shown in Fig. S3, but the interpretation of the results as shown in the main text using
205 all 23 models does not change.

206

207 **3 Results**

208 **3.1 Rio de Janeiro's spring 2023 heatwave**

209 The city of Rio de Janeiro experienced exceptionally high temperatures in both the
210 austral winter and spring of 2023, peaking on November 18 (Fig. 1). This record-breaking event
211 became the highest daily maximum temperature on record at the Galeão International Airport
212 weather station, reaching 41.3°C. The extreme heat event was also notable for its accompanying
213 high specific humidity, which rose alongside temperature in the days leading up to November 18
214 (Fig. 1b). The combination of elevated temperature and humidity rendered the event a humid
215 heat extreme, as measured by wet bulb temperature, which peaked at 28.2°C on November 18
216 (Fig. 1c). The coincidence of extreme dry and wet bulb temperatures is typical for extreme heat
217 events in Rio de Janeiro, where there is a statistically significant positive correlation between
218 daily maximum temperature and daily mean specific humidity (Fig. S4). This relationship is
219 facilitated by the city's abundant access to moisture from the coast and surrounding vegetation.



220

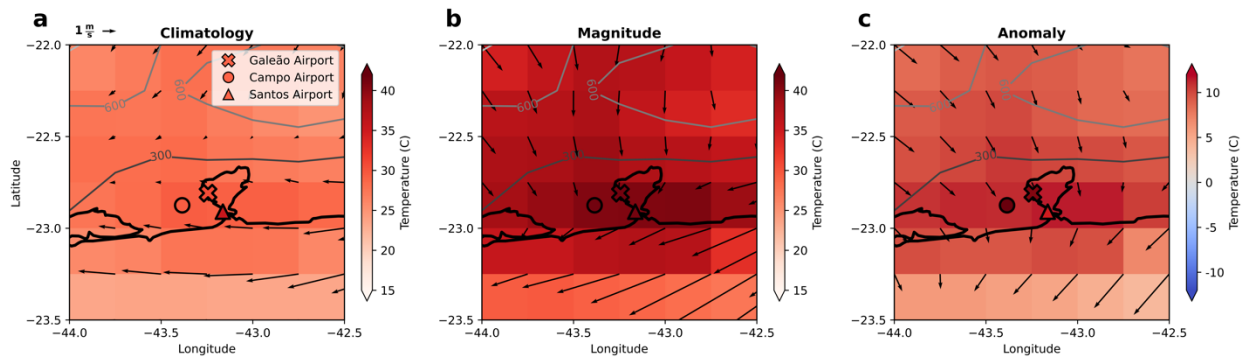
221 **Figure 1: Historical climatology and 2023 recorded a) daily maximum temperature, b)**
 222 **daily mean specific humidity, and c) daily maximum wet bulb temperature in the city of**
 223 **Rio de Janeiro. Data from the Galeão International Airport weather station as reported by**
 224 **the HadISD dataset. Vertical dashed line identifies record-breaking temperature event on**
 225 **November 18, 2023.**

226

227 Elevated temperatures occurred over an area greater than the city of Rio de Janeiro, but
 228 were spatially constrained by orography (Fig. 2). We explore the spatial patterns of the heatwave
 229 in data from the European Centre for Medium-Range Weather Forecasts (ERA5) reanalysis
 230 during the period of 1979-2023 (Hersbach et al., 2020). We see that hotspots in elevated

231 temperatures were located throughout the coastal region surrounding Rio de Janeiro, with sharp
 232 declines across the mountainous terrain moving inland. These positive coastal temperature
 233 anomalies coincide with northerly surface wind anomalies. ERA5 estimates the daily maximum
 234 temperature on November 18 in the grid cell containing the Galeão International Airport weather
 235 station as 40.6°C, within the range of temperatures recorded throughout weather stations in the
 236 city (Fig. 2c; Fig. S1). This extreme event was also remarkable in length as measured by ERA5,
 237 as daily maximum temperatures were above the locally defined 90th percentile for eight
 238 consecutive days, and above the 99th percentile for the final three days of this period (percentiles
 239 calculated from ERA5 across the period from 1979-2023). This multi-day interval of exceptional
 240 temperatures rendered it difficult for residents to find relief.

241



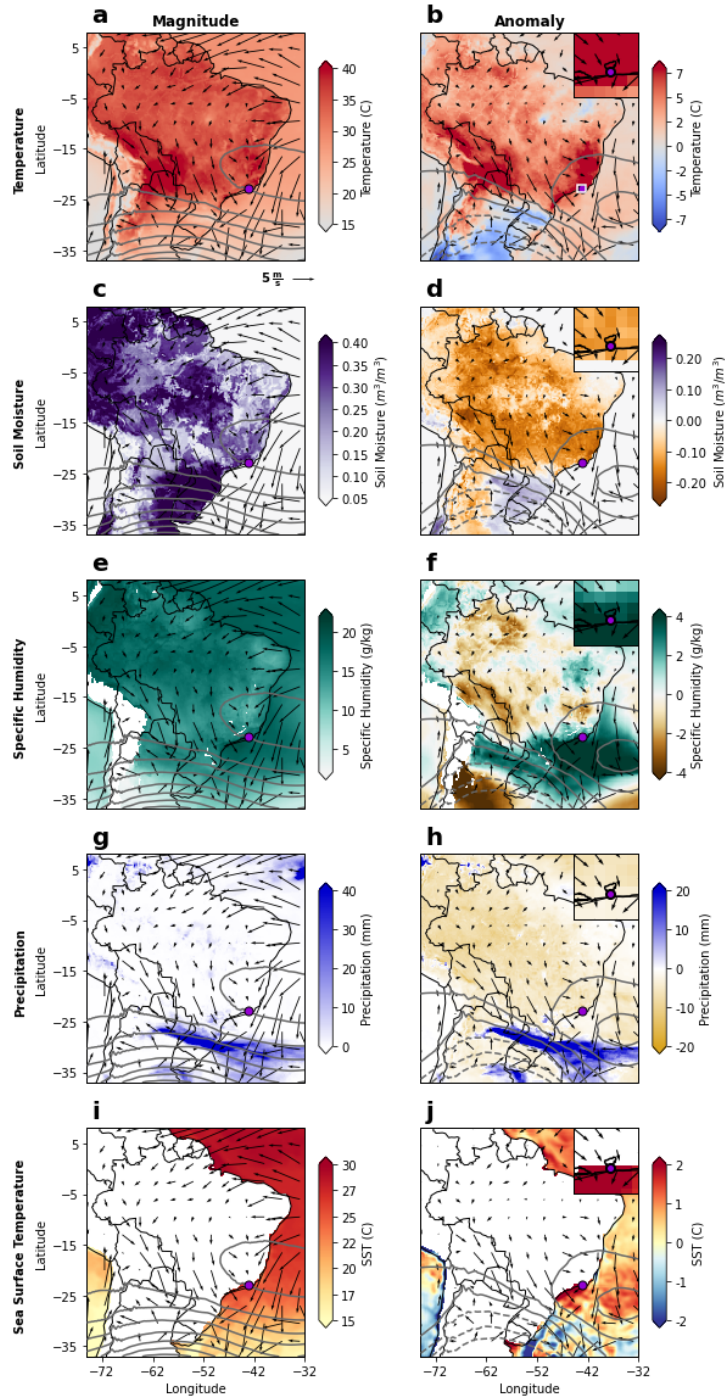
242

243 **Figure 2: Spatial maps of daily maximum temperatures during the date of peak extreme**
 244 **heat intensity in the city of Rio de Janeiro using ERA5 data (shading) and three city**
 245 **weather stations with long-term temperature records (markers). Vectors represent surface**
 246 **winds; contours represent elevation in meters. A) Climatology during November 18**
 247 **throughout the historical record. B) Magnitudes on November 18, 2023. C) Anomalies**
 248 **during November 18, 2023.**

249

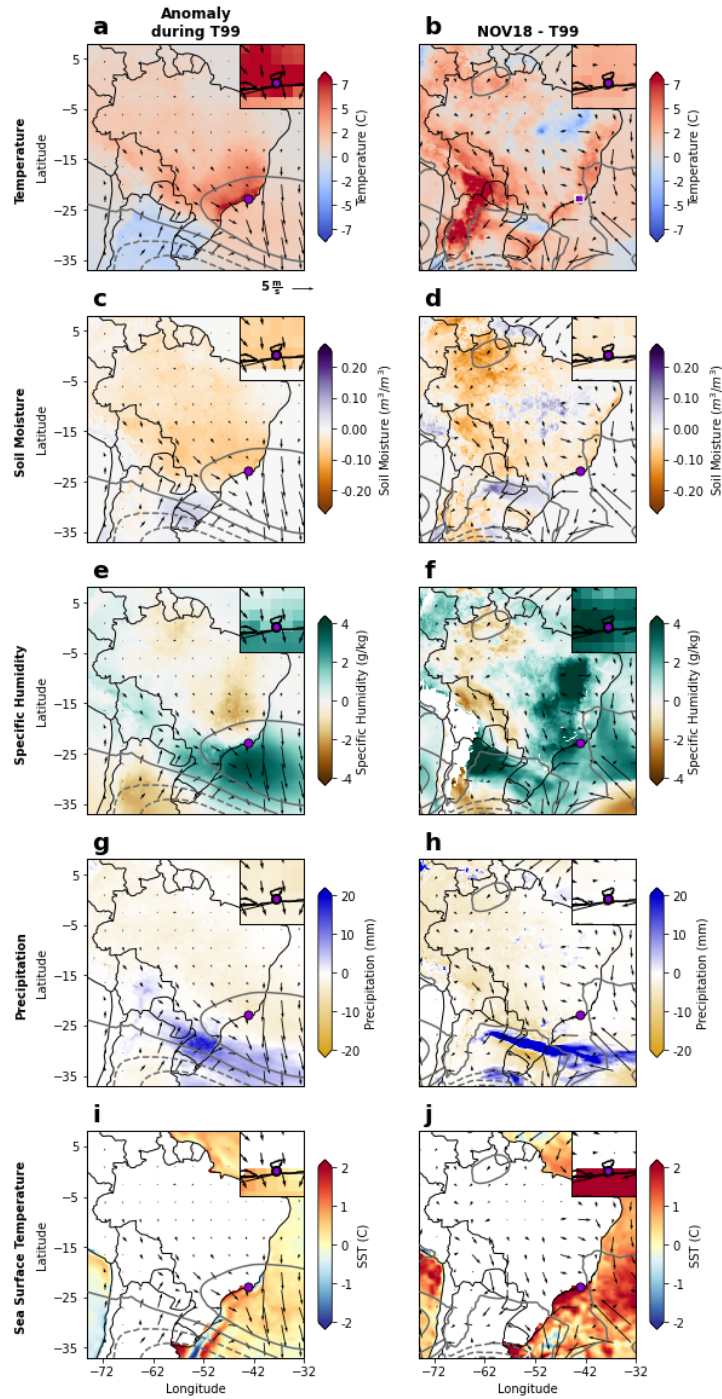
250 The maximum temperature during the event on November 18 coincided in time with
 251 other anomalous meteorological conditions (Fig. 3; for climatological values, see Fig. S5 in the
 252 Supplemental Materials). Positive geopotential height anomalies centered over Rio de Janeiro
 253 were consistent with an intensification of the South American Subtropical High, a semi-
 254 permanent anticyclonic circulation system off the Southeast coast of Brazil. The edge of this
 255 positive high pressure anomaly was collocated with the region of positive temperature anomalies
 256 that includes the city of Rio de Janeiro (Fig. 3b). Surface winds off the coast of Rio de Janeiro
 257 were anomalously northerly. Anomalously northerly flow in this mountainous area can

258 exacerbate high temperatures directly through downslope winds (Stefanello et al. 2022).
259 Previous literature has also shown that anomalously northerly winds over the coast can increase
260 local sea surface temperatures through reductions in wind-driven upwelling, reducing the
261 capacity for coastal cooling (Castelao and Barth 2006; Palma and Matano 2009). Indeed, positive
262 SST anomalies of up to 2°C occurred along Rio de Janeiro’s coast on the day of the peak in air
263 temperature (Fig. 3j). Anomalous winds over the interior of South America also enhanced the
264 northerly South American Low Level Jet (Marengo et al., 2004; Montini et al., 2019). Positive
265 specific humidity anomalies were present throughout Southeast and South Brazil (Fig. 3f),
266 intersecting with an area of precipitation along the edge of the low pressure system to the south
267 (Fig. 3g). The northern portion of the positive specific humidity anomaly was aligned with the
268 positive geopotential height anomaly off the coast of Southeast Brazil. Widespread negative soil
269 moisture anomalies occurred throughout most of Brazil, and the interior of South America more
270 broadly, during this event (Fig. 3d). The large spatial coverage of these negative soil moisture
271 anomalies was concurrent with Amazonian drought recorded during this time, inherited from the
272 prior season (Espinoza et al., 2024). These spatial patterns are typical of extreme heat events
273 during the spring season in the city of Rio de Janeiro, though the magnitudes of the anomalies in
274 all of these variables are dramatically higher on November 18, 2023 than during other spring
275 extreme heat events (Fig. 4). The most unique features of the November 18 event were the
276 intensified northerly winds and the degree of inland penetration of positive specific humidity
277 anomalies (Fig. 4e-f). Further, the positive local SST anomalies off the coast of Rio de Janeiro
278 were particularly exceptional in intensity and spatial scale during this event, weakening the sea-
279 air temperature contrast and sea-breeze (Fig. 4i-j). Outside of these specific distinctions, the
280 event on November 18, 2023 was an intense example of a typical spring extreme heat event in
281 the region.



282

283 **Figure 3: Magnitude (left) and anomalies (right) of daily maximum temperature, mean soil**
 284 **moisture, mean specific humidity, total precipitation, and mean SST on day of peak**
 285 **temperature in the city of Rio de Janeiro (November 18, 2023). Overlying wind vectors and**
 286 **500 hPa geopotential height contours (50 m and 25 m contour levels for magnitude and**
 287 **anomaly plots, respectively). Anomalies calculated relative to historical calendar date mean**
 288 **values across the period from 1979-2023. Inset in the upper right corner of each anomaly**
 289 **plot zooms in on the white box surrounding the city of Rio de Janeiro (purple marker) in**
 290 **the top right subplot.**

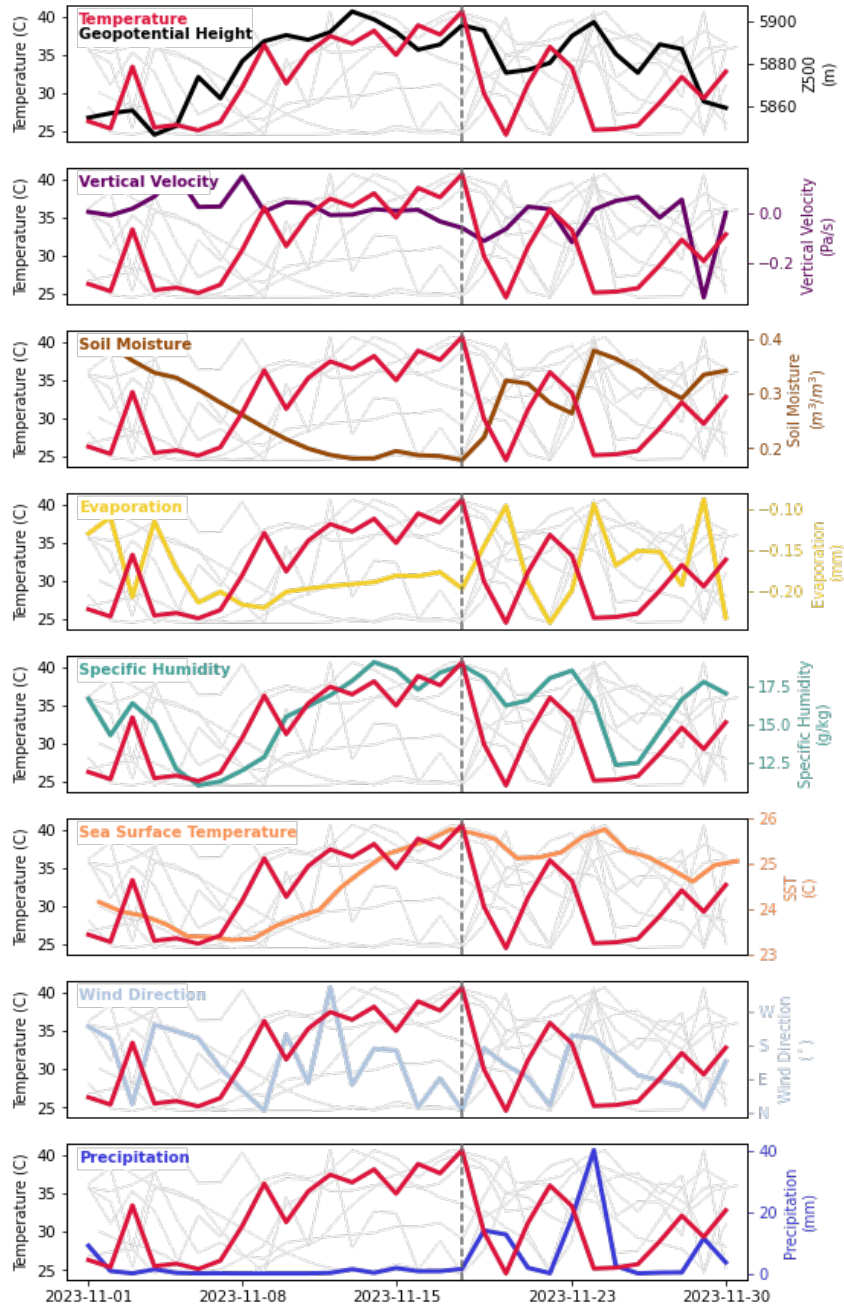


291

292 **Figure 4: Anomalies in daily maximum temperature, mean soil moisture, mean specific**
 293 **humidity, total precipitation, and mean SST during 99th percentile extreme temperature**
 294 **days in the September-November (SON) season for the ERA5 grid cell which includes the**
 295 **Galeão International Airport weather station (left). Difference in conditions on November**
 296 **18 compared to mean conditions during these 99th percentile extreme temperature days**
 297 **(right).**

298 The time evolution of the meteorological variables described above throughout the month
299 of November 2023 uncovers the temporal development of the extreme heat event (Fig. 5). Rising
300 temperatures throughout the weeks leading up to November 18 were preceded by elevated
301 geopotential heights at 500 hPa and associated atmospheric subsidence. This was accompanied
302 by a rapid decline in soil moisture which was likely facilitated by the increased solar insolation
303 associated with the persistent high pressure system and resulting extremely low precipitation
304 from November 2-November 18. Given that the rainy season in Southeast Brazil typically begins
305 in late-October to mid-November (Coelho et al., 2021; Latinovic et al., 2018; Marengo et al.,
306 2012; Liebmann and Mechoso 2011; Raia and Cavalcanti 2008), this period of consecutive dry
307 days was unusual. Indeed, this period totals 17 days in a row with less than 5 mm of rain per day,
308 and this only happened during the month of November in one other year in the historical record
309 from ERA5 between 1979-2023 (2012). These changes in geopotential height, soil moisture, and
310 suppressed precipitation preceded changes in other variables, evidenced by the grey lines in the
311 background of each subplot. Wind direction was highly variable on a daily scale, but became
312 increasingly northerly during this same period. These changes were accompanied by a gradual
313 increase in SST off the coast of Rio de Janeiro, though delayed compared to that of the local air
314 temperature. These changes in wind direction and SSTs are likely linked, as upwelling in this
315 region can be significantly reduced through northerly wind anomalies, increasing coastal sea
316 surface temperatures (Castelao and Barth 2006; Palma and Matano 2009). Secondary pathways
317 to SST increases could include increased solar radiation to the ocean, added heat flux to the
318 ocean, and a thinning of the oceanic mixed layer. These features are common around many
319 coastlines during atmospheric heatwaves that are associated with warming coastal waters, though
320 further research would be needed to quantify their relative importance during the November
321 2023 heatwave in Rio de Janeiro. As air temperatures rose, specific humidity increased over the
322 city. This was likely related to both local evaporation from the soil (co-occurring with declining
323 soil moisture) and moisture advected from the anomalously warm coastal waters and surrounding
324 vegetation. The circulation specifically on November 18 directed wind in the larger region
325 surrounding Rio de Janeiro to intensify the South American Low Level Jet, which can
326 additionally increase moisture transport from the Amazon Basin to Southeast Brazil (Marengo et
327 al., 2004; Vera et al., 2006; Montini et al., 2019). However, convergence of the horizontal
328 moisture flux at the level nearest the surface was only stronger than its climatological values in

329 some grid cells within the northern and western areas of the city (Fig. S6). More generally,
 330 specific humidity was also able to build without reaching saturation due to the increasing
 331 temperatures (and the Clausius-Clapeyron relation). Finally, the heatwave was terminated when
 332 a two-day precipitation event occurred from November 19- 20. This precipitation induced a
 333 small decline in specific humidity and SST, as well as a rapid increase in soil moisture.
 334



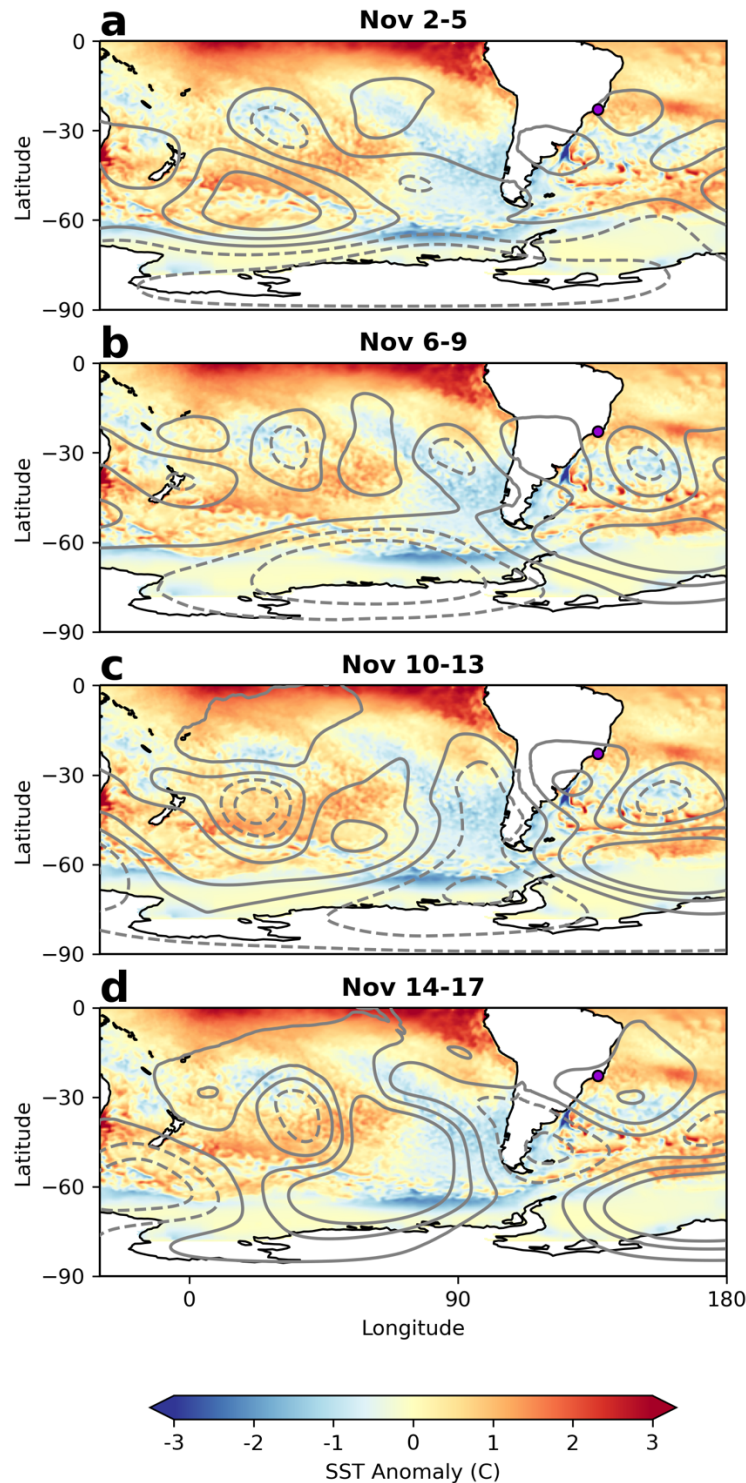
335

336 **Figure 5: Evolution of meteorological conditions during the month of November 2023 in**
337 **Rio de Janeiro. Grey lines in the background of each subplot show the evolution of all**
338 **variables, with individual variables compared in colors to dry bulb temperature in red.**
339 **Vertical dashed line identifies record-breaking temperature event on November 18, 2023.**
340 **All variables are calculated for the grid cell which includes the Galeão International**
341 **Airport weather station except SST, which is averaged over the box 21°S-24°S and 42°W-**
342 **45°E.**

343

344 The evolution of the 2023 heatwave as shown above is reminiscent of that during the
345 2010 heatwave analyzed by Geirinhas and coauthors (2019). Those authors explain that the
346 extreme heat event in the summer of 2010 was initiated by a positive SST anomaly over the
347 eastern Pacific that triggered a Rossby wave train that in turn intensified the South Atlantic
348 Subtropical High. Modulation of this climatological high pressure system has been shown to be
349 central to influencing weather in the city of Rio de Janeiro, and particularly temperatures there
350 (Geirinhas et al., 2018). Here we also observe a positive SST anomaly over the equatorial Pacific
351 throughout the month of November and a resulting anomalous wave pattern ending over the
352 South Atlantic High that became increasingly organized and strengthened during the two weeks
353 before November 18 (Fig. 6; see Fig. S7 in the Supplemental Materials for maps of the
354 climatologies and absolute magnitudes of these variables). This mechanism is similar to how El
355 Niño generally influences temperatures in Southeast Brazil on longer timescales (Cai et al.,
356 2020), and we confirm that there is a positive correlation between the ENSO state as quantified
357 by the Niño3.4 index and the frequency of high heat days in the city of Rio de Janeiro in the
358 austral spring season (Fig. S8). Further, the mean spatial SST and Z200 patterns during the
359 spring of typical El Niño years look very similar to those observed during November 2023,
360 though the anomalies in both SST and geopotential height are much larger during November
361 2023 (Figure S9). 2023 was characterized by a transition from La Niña to El Niño, with the El
362 Niño emerging in April-June 2023 and strengthening to a strong El Niño in the second half of
363 2023 (Becker et al., 2024). The SST anomalies associated with the El Niño could have been
364 responsible for initiating the wave train which set off the geopotential height anomalies over Rio
365 de Janeiro, consistent with the results of a recent analysis exploring spring and winter heatwaves
366 throughout South America during 2023 (Marengo et al. 2025). More broadly, it has been
367 suggested that multi-month elevations in temperature over Brazil throughout 2023 could be
368 driven in part by El Niño (Pampuch et al. 2025). Further, the second half of 2023 was

369 exceedingly warm globally (Cattiaux et al. 2024; Perkins-Kirkpatrick et al. 2024), due in large
370 part to anthropogenic warming, indicating that climate variability and climate change both likely
371 preconditioned the November 2023 extreme heat event. We note that similar wave trains driven
372 by Pacific SST anomalies have been shown to influence weather in Southeast Brazil even during
373 neutral ENSO states (Seth et al., 2015). Additionally, the instantaneous extreme temperature
374 event and the preceding persistent dry conditions must also be linked to the synoptic weather in
375 the area. Decreases in soil moisture and horizontal moisture fluxes by intensification of the South
376 American Low Level Jet were central features of the heatwave in 2010, as they were in
377 November 2023. These overlaps in the apparent drivers of the 2010 and 2023 heatwaves
378 underscore that while the 2023 spring event was unprecedented in its magnitude and unusual in
379 its spring timing, it was not unique in its overall dynamics.



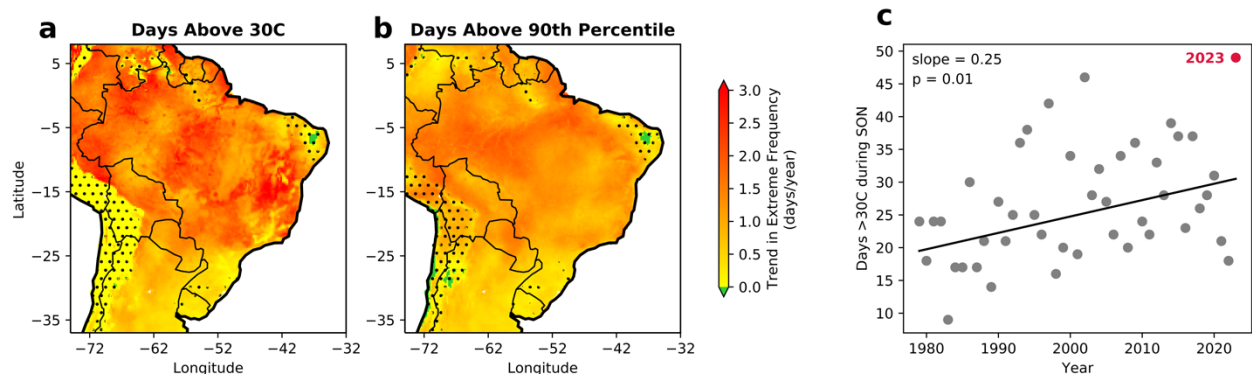
380

381 **Figure 6: Evolution of the geopotential height at 200 hPa (contours) in the weeks of**
 382 **suppressed precipitation leading up to the extreme heat event on November 18 in the city of**
 383 **Rio de Janeiro. Geopotential height anomaly contour levels are at 100 m, with positive**
 384 **(negative) anomalies in solid (dashed) contours. Across all subplots, shading indicates**
 385 **November 2023 mean SST anomalies.**

386

387 3.2 Historical and future changes in extreme heat

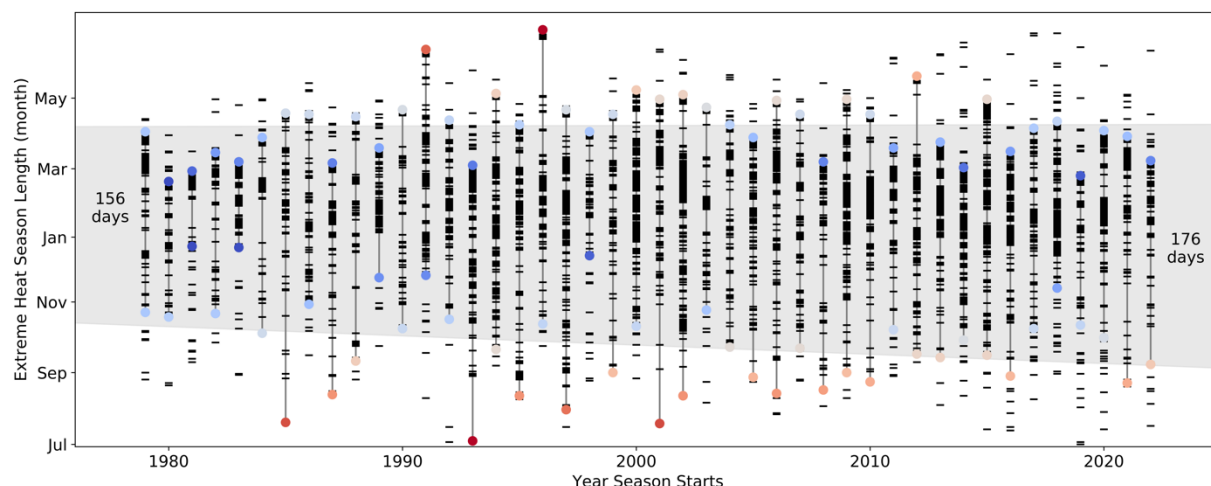
388 Extreme heat events have become more frequent in the city of Rio de Janeiro and the
389 timing of these events has shifted earlier in the calendar year. There has been a significant
390 increase in the number of days above 30°C each year over the past 44 years throughout almost
391 all of South America (Fig. 7a). Further, the number of 90th percentile days locally defined at each
392 grid cell has also increased significantly throughout most of the region (Fig. 7b). In the city of
393 Rio de Janeiro specifically, the number of 30°C days per year during the austral spring is
394 increasing at a rate of 0.27 days/year (Fig. 7c). Relative to 1979, the city now experiences almost
395 12 additional days per year above 30°C during the spring season alone. Overall, the extreme heat
396 season in Rio de Janeiro is broadening. As measured by the number of days between the first and
397 last heatwave day of the season (a period of three or more consecutive days with daily maximum
398 temperatures above 31.4°C), the extreme heat season has lengthened from 156 days in the 1979-
399 1980 season to 176 days in the 2022-2023 season (Fig. 8). The broadening of the heat season is
400 due primarily to more early season heatwave days, while the end date of the heat season has not
401 changed significantly.



402

403 **Figure 7: Historical trend from 1979-2023 in the number of days per year above a) 30°C**
404 **and b) locally defined 90th percentile. Stippling shows areas which are not significant at a p**
405 **= 0.05 level assessed using a Wald Test. c) Trend in number of days per year above 30°C**
406 **taking place in the SON season in ERA5 for the grid cell which includes the Galeão**
407 **International Airport weather station.**

408

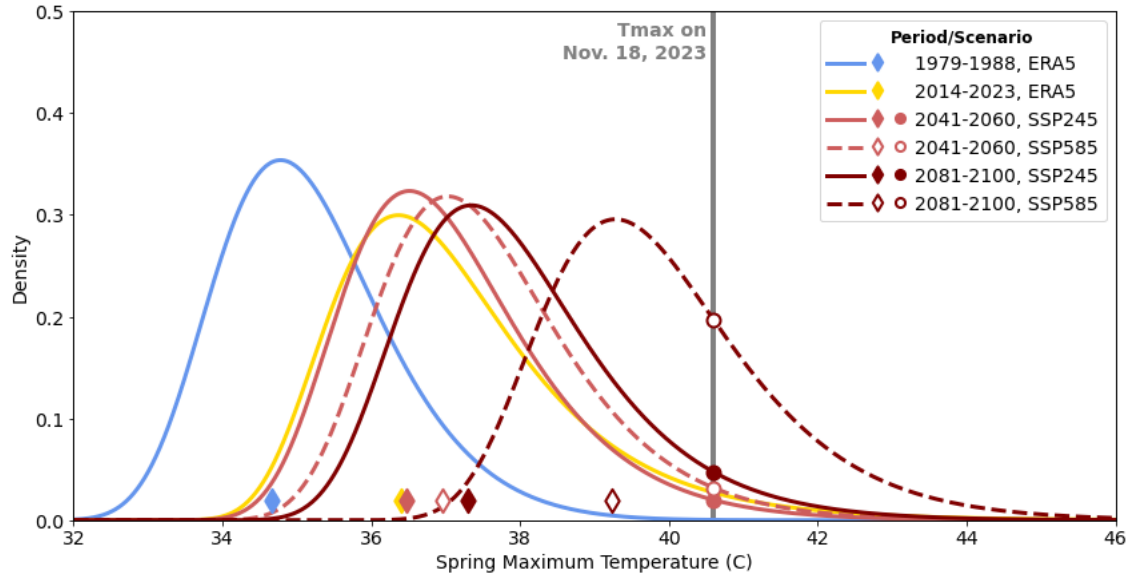


409
 410 **Figure 8: Shifting timing of the city of Rio de Janeiro extreme heat season. Horizontal axis**
 411 **indicates the year in which winter begins (“January” marking denotes the start of the**
 412 **following calendar year). Colored markers indicate the first and last days of the extreme**
 413 **heat season each year. Marker color indicates whether the start/end date is lengthening**
 414 **(red) or shortening (blue) the heat season compared to historical mean start/end dates.**
 415 **Dashes indicate individual additional days with daily maximum temperatures surpassing**
 416 **31.4°C (no persistence required). Grey shading indicates area between trend lines in the**
 417 **shifting seasonality.**

418
 419 The distribution of maximum spring temperatures in the city of Rio de Janeiro has shifted
 420 higher over the last four decades and this pattern is projected to continue in the future. In order to
 421 evaluate whether the observed historical increase in extreme heat frequency identified in Figures
 422 7 and 8 may continue in the future, we fit annual maximum spring temperatures from historical
 423 ERA5 reanalysis data and future projections from bias-corrected NASA Earth Exchange Global
 424 Daily Downscaled Projections (NEXGDDP) data (Thrasher et al., 2022, see Methods) to a
 425 Generalized Extreme Value (GEV) distribution. When comparing early and late historical
 426 periods from 1979-1988 and 2014-2023, respectively, the location parameter of the two GEV
 427 distributions has increased by 1.7°C (Fig. 9). The distribution of maximum austral spring
 428 temperatures in the city of Rio de Janeiro is also projected to continue shifting to higher values in
 429 the future, but the magnitude of this change is strongly dependent upon the future emissions
 430 pathway. The temperature distributions associated with mid-century periods (2041-2060) under
 431 SSP2-4.5 and SSP5-8.5 future scenarios are similar to that of the last 10 years of observational
 432 data, with shifts in the location parameters of 0.1°C and 0.9°C for the two emissions trajectories,

433 respectively. A larger change is projected by the end of the century (2081-2100) under each
434 emissions scenario. However, the end-of-century SSP5-8.5 scenario is distinctly separate from
435 the other distributions, with the distribution location parameter 2.8°C higher than during the last
436 10 years.

437 These changes to the distributions strongly influence the probability of an event with the
438 intensity of the maximum temperature recorded on November 18, 2023. The probability density
439 function fit to the projected annual maximum spring temperatures under each mid-century period
440 using a GEV distribution yields a return period for an extreme temperature event with the daily
441 maximum temperature at least 40.6°C in the city of Rio de Janeiro (analogous to the event on
442 November 18, 2023 as measured by ERA5) of 51 years under SSP2-4.5 and 33 years under
443 SSP5-8.5. By the end of the century under either emissions scenario, an event of this magnitude
444 becomes much more likely, with return periods of 19 years or just 4 years under SSP2-4.5 and
445 SSP5-8.5, respectively. These return periods align well with estimates for station-level
446 projections from Collazo et al. 2025, which estimates a return period of 4 to 9 years for
447 heatwaves analogous to that of November 2023 for a future climate with global mean surface
448 temperatures 2°C warmer than preindustrial levels. Recent literature has suggested that the
449 SSP5-8.5 scenario may not be realistic given our current socioeconomic, political, and physical
450 landscape (Hausfather and Peters 2020; Burgess et al., 2020; Ritchie and Dowlatabadi 2017).
451 However, these results indicate that an austral spring heatwave of the magnitude experienced in
452 the city of Rio de Janeiro on November 18 is projected to become much more frequent in the
453 future, even under the more stringent SSP2-4.5 emission pathway. As temperatures rise and the
454 city of Rio de Janeiro maintains its ample moisture sources from the nearby ocean and
455 vegetation, we expect that humid heat extremes will also become more frequent and intense,
456 though at a slower rate than dry bulb temperature extremes as dictated by tropical atmospheric
457 dynamics (Coffel et al. 2018; Zhang et al., 2021; Matthews et al., 2025). We must also note that
458 it is difficult to evaluate whether the models are missing emerging factors that could increase the
459 frequency and intensity of these extreme heat events – such as Amazonian deforestation or
460 declines in sea ice – reducing their ability to capture the possible future spring temperature
461 distributions in Rio de Janeiro.



462

463 **Figure 9: Generalized Extreme Value distributions for SON maximum temperatures**
 464 **during early and late historical periods (observed in ERA5), mid-century periods, and end-**
 465 **of-century periods under SSP2-4.5 and SSP5-8.5 (projections from bias-corrected**
 466 **NEXGDDP data). Diamonds indicate the value of the location parameter for each**
 467 **distribution. Vertical grey line shows the magnitude of the extreme temperature event on**
 468 **November 18, 2023.**

469

470 **4 Conclusions**

471 The November 2023 heatwave in the city of Rio de Janeiro was a record-breaking event
 472 characterized by meteorological conditions largely typical of spring extreme temperature events,
 473 but exceptional in their magnitudes. Rising temperatures were associated with positive
 474 geopotential height anomalies and corresponding atmospheric subsidence which facilitated clear
 475 sky conditions and increased sensible heat flux at the surface. These high pressure anomalies
 476 centered over the South Atlantic Subtropical High were likely related to the strong 2023-24 El
 477 Niño event. The subsidence near Rio de Janeiro associated with the geopotential height
 478 anomalies also suppressed precipitation and facilitated evaporation from the land surface, leading
 479 to decreased soil moisture and increased specific humidity. Moisture was available from multiple
 480 sources to facilitate these humidity increases, as Rio de Janeiro is a coastal city and downwind of
 481 both the Amazon and more local vegetation. SSTs off the coast of Rio de Janeiro were also
 482 highly elevated in the days before the heatwave peak, reducing the potential for coastal cooling.
 483 Finally, the event was terminated on November 19 due to the evaporative cooling, shading, and
 484 mixing associated with the onset of precipitation. The combination of changes in circulation,

485 land surface feedbacks, and atmosphere-ocean interactions generated the conditions for an
486 exceptionally intense and persistent extreme heat event in the city of Rio de Janeiro.

487 The risk of extreme heat in austral spring is increasing significantly in Rio de Janeiro. We
488 find that extreme spring temperature events are becoming more frequent and that the extreme
489 heat season is starting earlier and lasting longer than in previous decades. Further, extreme heat
490 of the magnitude on November 18, 2023 may become much more likely by mid- and end-of-
491 century periods. However, the absolute increase in the frequency of similar heatwaves is largely
492 dependent upon our future emissions pathway.

493 The November 2023 heatwave had devastating impacts, including loss of life. As our
494 climate continues to change and extreme heat in the city of Rio de Janeiro continues to increase
495 in intensity and frequency, we can expect more strain on human health and cascading
496 socioeconomic impacts. This extreme heat event was exceptional not only in its intensity, but
497 also in its persistence. Consecutive extreme heat days have been shown to have nonlinear
498 impacts on human health, in Brazil and in other countries, as they prevent individuals, buildings,
499 and critical electrical equipment from cooling down between heat events (Geirinhas et al., 2020;
500 Baldwin et al., 2019). More broadly, the direct impacts of heatwaves on hospitalizations
501 throughout Brazil have been documented, with the largest effects occurring in long duration
502 events (Zhao et al., 2019). These impacts of heatwaves on mortality are projected to increase,
503 with particular consequences for elderly populations, especially if targeted adaptation measures
504 are not put in place (Diniz et al., 2020). Continuing to improve our understanding of how and
505 when extreme heat occurs is thus essential as our climate continues to change. This is
506 particularly true for locations such as Rio de Janeiro, which historically has not been a hotspot of
507 extreme heat – especially in the shoulder seasons – and thus individuals may not be well
508 acclimated to extreme temperatures then (Periard et al., 2015; Horowitz 2016). The human health
509 impacts of unusually intense events may be exacerbated by the shifting timing of extreme heat,
510 as record-breaking exceptional heat events are now occurring outside of the traditional extreme
511 heat season when individuals may not be prepared to utilize heat mitigation strategies (De Freitas
512 & Grigorieva, 2015). Because Rio de Janeiro is an area of emerging risk for extreme heat, further
513 research on models’ ability to capture the historical drivers and timing of heatwaves in this
514 region and evaluations of how these characteristics might shift in the future should be pursued.

515 The meteorological conditions surrounding the extreme heat event analyzed here
516 demonstrate the potential for compound hazards throughout Brazil. The identified circulation
517 pattern that establishes the atmospheric blocking associated with heatwaves in Rio de Janeiro is
518 also likely linked to heavy precipitation events in South Brazil, an extreme case of which
519 occurred in May 2024 in center-north of Rio Grande do Sul, including the metropolitan area of
520 Porto Alegre, displacing hundreds of thousands and killing at least 155 people (Rogerio 2024).
521 The temporal compounding of these extreme temperature and flooding events within Brazil has
522 the potential to strain the country’s disaster management systems more than events occurring in
523 isolation. Furthermore, the exceptional spatial area within Brazil that experienced anomalous
524 heat in the November 2023 event, relative to 99th percentile heat events in the city of Rio de
525 Janeiro, underscores the potential for spatially compounding heat that could lead to outsized
526 impacts. Exploring how unprecedented global surface ocean and surface temperatures, along
527 with regional features like the broader heat and drought across much of Brazil, may contribute to
528 extreme heat in the city of Rio de Janeiro will be an important component to improving our
529 understanding of these compound events’ drivers, prediction capacity, and potential to change in
530 the future.

531 The evolving meteorological conditions associated with this heatwave were strongly
532 impacted by the lack of precipitation in the first two weeks of November. This is particularly
533 unexpected due to the fact that the active phase of the South American Monsoon System
534 typically begins in late October or early November in this region (Marengo et al., 2012;
535 Liebmann and Mechoso 2011; Raia and Cavalcanti 2008), which is linked to an increase in
536 convective activity in tropical South America in the warm season (Jones and Carvalho 2013).
537 Observational and modeling studies suggest that the South American Monsoon System dry
538 season is lengthening (Arias et al., 2015; Fu et al., 2013) and that the onset of the active phase is
539 delaying (Gomes et al., 2022; Pascale et al., 2019). These trends are projected to continue to
540 some degree in the future with further climate change, particularly in light of ongoing
541 deforestation which contributes to regional drying trends in the Amazon and other areas of Brazil
542 (Boisier et al., 2015; Swann et al., 2015). Given Rio de Janeiro is a city with abundant access to
543 moisture due to its proximity to the coast and vegetation, the increasingly constrained active
544 monsoon phase could lead to increased frequency and intensity of extreme humid heat in the
545 spring season (Ivanovich et al., 2024). These changes could be responsible for the evident

546 asymmetrical historical increase in heat season length during the spring versus fall as
547 demonstrated here, and extensions of this work should be devoted to an exploration of these
548 potential relationships.

549 This work highlights the challenge of analyzing the drivers of weather extremes in such a
550 climatically diverse city as Rio de Janeiro and emphasizes the need for future research to explore
551 high resolution comparisons of mechanisms controlling the city's microclimates. Differences
552 between conditions recorded at individual weather stations within the city's boundaries
553 demonstrate the degree to which the dynamics of events in each neighborhood depend on the
554 station's location relative to the coast versus interior (Raymond and Mankin 2019), elevation
555 (Raymond et al., 2022; Pepin et al., 2015), and degree of urbanization (Kruger et al., 2024;
556 Chakraborty et al., 2022; Tan et al., 2010). Higher temporal resolution analysis would also better
557 capture sub-daily processes such as sea breeze and their effect on extreme heat throughout the
558 city. Further, many of these mechanisms influencing the intracity variability of heat stress
559 exposure only focus on the effect of differences in dry bulb temperature. Factoring in the spatial
560 variation in humidity, solar insolation, and windspeed complicate understanding, but are
561 essential for capturing humans' exposure to heat stress conditions. These intracity differences
562 also meaningfully impact compound events with non-heat environmental hazards, such as floods,
563 landslides, droughts, and air pollution, as well as how exposure to these hazards intersects with
564 areas of social vulnerability. Future work should be devoted to investigating the different
565 magnitudes of extreme heat and controlling mechanisms throughout Rio de Janeiro in order to
566 inform targeted extreme heat adaptation plans for individual neighborhoods within the city.

567
568 *Data Availability:* The publicly available datasets used in this analysis are accessible via the
569 following websites: HadISD, <https://www.metoffice.gov.uk/hadobs/hadis/>; ERA5,
570 <https://cds.climate.copernicus.eu/datasets/reanalysis-era5-single-levels?tab=overview> and
571 <https://cds.climate.copernicus.eu/datasets/reanalysis-era5-pressure-levels?tab=overview>; OISST,
572 <https://www.ncei.noaa.gov/products/optimum-interpolation-sst>; and NEXGDDP,
573 <https://www.nccs.nasa.gov/services/data-collections/land-based-products/nex-gddp-cmip6>.
574 Station data from the Rio Alert System will be uploaded and accessible via a GitHub repository
575 upon manuscript publication.

576

577 *Code Availability:* All code used for the derivations, calculations, and data visualization will be
578 made publicly available via a GitHub repository upon manuscript publication.

579

580 *Author Contributions:*

581 S.J.C. conceived of the initial project concept. All co-authors contributed to study design, and
582 C.I. performed the analysis. C.I. wrote the initial manuscript draft with the feedback and
583 interpretation of all co-authors. All co-authors read and edited the manuscript.

584

585 *Competing Interests:*

586 The authors declare that they have no conflict of interest.

587

588 *Acknowledgements:*

589 This work was partially supported and funded by Columbia Global at Columbia University,
590 “Simulation of Extreme Weather Events in Brazilian Megacities”, a Climate Hub | Rio Project.
591 Climate Hub | Rio is a knowledge, research, and innovation hub that brings together experts from
592 Brazil, Columbia University, and around the world to advance climate-related knowledge and
593 action in Rio and Brazil. Direct funding for C. Ivanovich and R. Horton was provided by
594 National Oceanic and Atmospheric Administration’s Regional Integrated Sciences and
595 Assessments program, Grant NA15OAR4310147. A. H. Sobel acknowledges support from NSF
596 Grant AGS-1933523. S. J. Camargo is partially supported by the NOAA grant
597 NA23OAR43201600. The authors declare no competing interests.

598 **References**

- 599 Alvares, C. A., Stape, J. L., Sentelhas, P. C., & De Moraes Gonçalves, J. L. (2013). Modeling
600 monthly mean air temperature for Brazil. *Theoretical and Applied Climatology*, 113(3–
601 4), 407–427. <https://doi.org/10.1007/s00704-012-0796-6>
- 602 Alvarez, M. S., Vera, C. S., Kiladis, G. N., & Liebmann, B. (2016). Influence of the Madden
603 Julian Oscillation on precipitation and surface air temperature in South America. *Climate*
604 *Dynamics*, 46(1), 245–262. <https://doi.org/10.1007/s00382-015-2581-6>
- 605 Arias, P. A., Fu, R., Vera, C., & Rojas, M. (2015). A correlated shortening of the North and
606 South American monsoon seasons in the past few decades. *Climate Dynamics*, 45(11),
607 3183–3203. <https://doi.org/10.1007/s00382-015-2533-1>
- 608 Baldwin, J. W., Dessy, J. B., Vecchi, G. A., & Oppenheimer, M. (2019). Temporally Compound
609 Heat Wave Events and Global Warming: An Emerging Hazard. *Earth’s Future*, 7(4),
610 411–427. <https://doi.org/10.1029/2018EF000989>
- 611 Becker, E., L’Heureux, M., Hu, Z.-Z., & Kumar, A. (2024). ENSO and the tropical Pacific. In
612 “State of the Climate in 2023”. *Bull. Amer. Meteor. Soc.*, 105 (8), S221-S224,
613 <https://doi.org/10.1175/BAMS-D-24-0098.1>
- 614 Bitencourt, Daniel P., Fuentes, M. V., Franke, A. E., Silveira, R. B., & Alves, M. P. A. (2020).
615 The climatology of cold and heat waves in Brazil from 1961 to 2016. *International*
616 *Journal of Climatology*, 40(4), 2464–2478. <https://doi.org/10.1002/joc.6345>
- 617 Bitencourt, Daniel Pires, Muniz Alves, L., Shibuya, E. K., De Ângelo Da Cunha, I., & Estevam
618 De Souza, J. P. (2021). Climate change impacts on heat stress in Brazil—Past, present,
619 and future implications for occupational heat exposure. *International Journal of*
620 *Climatology*, 41(S1). <https://doi.org/10.1002/joc.6877>
- 621 Boisier, J. P., Ciais, P., Ducharne, A., & Guimberteau, M. (2015). Projected strengthening of
622 Amazonian dry season by constrained climate model simulations. *Nature Climate*
623 *Change*, 5(7), 656–660. <https://doi.org/10.1038/nclimate2658>
- 624 Burgess, M. G., Ritchie, J., Shapland, J., & Pielke, R. (2020). IPCC baseline scenarios have
625 over-projected CO2 emissions and economic growth. *Environmental Research Letters*,
626 16(1), 014016. <https://doi.org/10.1088/1748-9326/abcedd2>
- 627 Cai, W., McPhaden, M. J., Grimm, A. M., Rodrigues, R. R., Taschetto, A. S., Garreaud, R. D., et
628 al., (2020). Climate impacts of the El Niño–Southern Oscillation on South America.

629 Nature Reviews Earth & Environment, 1(4), 215–231. <https://doi.org/10.1038/s43017->
630 020-0040-3

631 Castelao, R. M., & Barth, J. A. (2006). Upwelling around Cabo Frio, Brazil: The importance of
632 wind stress curl. *Geophysical Research Letters*, 33(3), 2005GL025182.
633 <https://doi.org/10.1029/2005GL025182>

634 Cattiaux, J., Ribes, A., & Cariou, E. (2024). How Extreme Were Daily Global Temperatures in
635 2023 and Early 2024? *Geophysical Research Letters*, 51(19), e2024GL110531.
636 <https://doi.org/10.1029/2024GL110531>

637 Chakraborty, T., Venter, Z. S., Qian, Y., & Lee, X. (2022). Lower Urban Humidity Moderates
638 Outdoor Heat Stress. *AGU Advances*, 3(5), e2022AV000729.
639 <https://doi.org/10.1029/2022AV000729>

640 Cheng, Y.-T., Lung, S.-C. C., & Hwang, J.-S. (2019). New approach to identifying proper
641 thresholds for a heat warning system using health risk increments. *Environmental*
642 *Research*, 170, 282–292. <https://doi.org/10.1016/j.envres.2018.12.059>

643 Cirino, P. H., Féres, J. G., Braga, M. J., & Reis, E. (2015). Assessing the Impacts of ENSO-
644 related Weather Effects on the Brazilian Agriculture. *Procedia Economics and Finance*,
645 24, 146–155. [https://doi.org/10.1016/S2212-5671\(15\)00635-8](https://doi.org/10.1016/S2212-5671(15)00635-8)

646 Coelho, C. A. S., De Souza, D. C., Kubota, P. Y., Cavalcanti, I. F. A., Baker, J. C. A.,
647 Figueroa, S. N., et al., (2022). Assessing the representation of South American monsoon
648 features in Brazil and U.K. climate model simulations. *Climate Resilience and*
649 *Sustainability*, 1(1), e27. <https://doi.org/10.1002/cli2.27>

650 Coffel, E. D., Horton, R. M., & de Sherbinin, A. (2018). Temperature and humidity based
651 projections of a rapid rise in global heat stress exposure during the 21st century.
652 *Environmental Research Letters*, 13(1), 014001. <https://doi.org/10.1088/1748->
653 9326/aaa00e

654 Collazo, S., Barriopedro, D., García-Herrera, R., & Beguería, S. (2025). Extreme heat and
655 mortality in the state of Rio de Janeiro in November 2023: attribution to climate change
656 and ENSO. *Natural Hazards and Earth System Sciences*, 25(9), 3221–3238.
657 <https://doi.org/10.5194/nhess-25-3221-2025>

658 Collins, J. M., Chaves, R. R., & Marques, V. da S. (2009). Temperature Variability over South
659 America. *Journal of Climate*, 22(22), 5854–5869.
660 <https://doi.org/10.1175/2009JCLI2551.1>

661 Cordero Simões dos Reis, N., Boiaski, N. T., & Ferraz, S. E. T. (2019). Characterization and
662 Spatial Coverage of Heat Waves in Subtropical Brazil. *Atmosphere*, 10(5), 284.
663 <https://doi.org/10.3390/atmos10050284>

664 Correio Braziliense. (2023, November 18). Rio bate recorde de calor do ano neste sábado (18/11)
665 com 42,5°C. Retrieved May 14, 2024, from
666 [https://www.correio braziliense.com.br/brasil/2023/11/6657444-rio-bate-recorde-de-calor-](https://www.correio braziliense.com.br/brasil/2023/11/6657444-rio-bate-recorde-de-calor-do-ano-neste-sabado-18-11-com-425-c.html)
667 [do-ano-neste-sabado-18-11-com-425-c.html](https://www.correio braziliense.com.br/brasil/2023/11/6657444-rio-bate-recorde-de-calor-do-ano-neste-sabado-18-11-com-425-c.html)

668 De Freitas, C., & Grigorieva, E. (2015). Role of Acclimatization in Weather-Related Human
669 Mortality During the Transition Seasons of Autumn and Spring in a Thermally Extreme
670 Mid-Latitude Continental Climate. *International Journal of Environmental Research and*
671 *Public Health*, 12(12), 14974–14987. <https://doi.org/10.3390/ijerph121214962>

672 Dereczynski, C., Silva, W. L., & Marengo, J. (2013). Detection and Projections of Climate
673 Change in Rio de Janeiro, Brazil, 2013. <https://doi.org/10.4236/ajcc.2013.21003>

674 Diniz, F. R., Gonçalves, F. L. T., & Sheridan, S. (2020). Heat Wave and Elderly Mortality:
675 Historical Analysis and Future Projection for Metropolitan Region of São Paulo, Brazil.
676 *Atmosphere*, 11(9), 933. <https://doi.org/10.3390/atmos11090933>

677 Dunn, R. J. H. (2019). HadISD version 3: monthly updates. Hadley Centre Technical Note.

678 Espinoza, J.-C., Jimenez, J. C., Marengo, J. A., Schongart, J., Ronchail, J., Lavado-Casimiro, W.,
679 & Ribeiro, J. V. M. (2024). The new record of drought and warmth in the Amazon in
680 2023 related to regional and global climatic features. *Scientific Reports*, 14(1), 8107.
681 <https://doi.org/10.1038/s41598-024-58782-5>

682 Feron, S., Cordero, R. R., Damiani, A., Llanillo, P. J., Jorquera, J., Sepulveda, E., et al., (2019).
683 Observations and Projections of Heat Waves in South America. *Scientific Reports*, 9(1),
684 8173. <https://doi.org/10.1038/s41598-019-44614-4>

685 Fu, R., Yin, L., Li, W., Arias, P. A., Dickinson, R. E., Huang, L., et al., (2013). Increased dry-
686 season length over southern Amazonia in recent decades and its implication for future
687 climate projection. *Proceedings of the National Academy of Sciences*, 110(45), 18110–
688 18115. <https://doi.org/10.1073/pnas.1302584110>

689 Geirinhas, J. L., Russo, A. C., Libonati, R., Miralles, D. G., Sousa, P. M., Wouters, H., & Trigo,
690 R. M. (2022). The influence of soil dry-out on the record-breaking hot 2013/2014
691 summer in Southeast Brazil. *Scientific Reports*, 12(1), 5836.
692 <https://doi.org/10.1038/s41598-022-09515-z>

693 Geirinhas, João L., Trigo, R. M., Libonati, R., Coelho, C. A. S., & Palmeira, A. C. (2018).
694 Climatic and synoptic characterization of heat waves in Brazil. *International Journal of*
695 *Climatology*, 38(4), 1760–1776. <https://doi.org/10.1002/joc.5294>

696 Geirinhas, João L., Trigo, R. M., Libonati, R., Castro, L. C. O., Sousa, P. M., Coelho, C. A. S., et
697 al., (2019). Characterizing the atmospheric conditions during the 2010 heatwave in Rio
698 de Janeiro marked by excessive mortality rates. *Science of The Total Environment*, 650,
699 796–808. <https://doi.org/10.1016/j.scitotenv.2018.09.060>

700 Geirinhas, João L., Russo, A., Libonati, R., Trigo, R. M., Castro, L. C. O., Peres, L. F., et al.,
701 (2020). Heat-related mortality at the beginning of the twenty-first century in Rio de
702 Janeiro, Brazil. *International Journal of Biometeorology*, 64(8), 1319–1332.
703 <https://doi.org/10.1007/s00484-020-01908-x>

704 Geirinhas, João L., Russo, A., Libonati, R., Sousa, P. M., Miralles, D. G., & Trigo, R. M. (2021).
705 Recent increasing frequency of compound summer drought and heatwaves in Southeast
706 Brazil. *Environmental Research Letters*, 16(3), 034036. [https://doi.org/10.1088/1748-](https://doi.org/10.1088/1748-9326/abe0eb)
707 [9326/abe0eb](https://doi.org/10.1088/1748-9326/abe0eb)

708 Gomes, G.D., Nunes, A.M.B., Libonati, R., & Ambrizzi, T. (2022). Projections of subcontinental
709 changes in seasonal precipitation over the two major river basins in South America under
710 an extreme climate scenario. *Climate Dynamics*, 58, 1147–1169.
711 <https://doi.org/10.1007/s00382-021-05955-x>

712 Grimm, A. M. (2019). Madden–Julian Oscillation impacts on South American summer monsoon
713 season: precipitation anomalies, extreme events, teleconnections, and role in the MJO
714 cycle. *Climate Dynamics*, 53(1), 907–932. <https://doi.org/10.1007/s00382-019-04622-6>

715 Hausfather, Z., & Peters, G. P. (2020). Emissions – the ‘business as usual’ story is misleading.
716 *Nature*, 577(7792), 618–620. <https://doi.org/10.1038/d41586-020-00177-3>

717 He, Z., Dai, A., & Vuille, M. (2021). The Joint Impacts of Atlantic and Pacific Multidecadal
718 Variability on South American Precipitation and Temperature. *Journal of Climate*,
719 34(19), 7959–7981. <https://doi.org/10.1175/JCLI-D-21-0081.1>

720 Hersbach, H., Bell, B., Berrisford, P., Hirahara, S., Horányi, A., Muñoz-Sabater, J., et al., (2020).
721 The ERA5 global reanalysis. *Quarterly Journal of the Royal Meteorological Society*,
722 146(730), 1999–2049. <https://doi.org/10.1002/qj.3803>

723 Horowitz, M. (2016). Epigenetics and cytoprotection with heat acclimation. *Journal of Applied*
724 *Physiology* (Bethesda, Md.: 1985), 120(6), 702–710.
725 <https://doi.org/10.1152/jappphysiol.00552.2015>

726 Huang, B., Liu, C., Banzon, V., Freeman, E., Graham, G., Hankins, B., et al., (2021).
727 Improvements of the Daily Optimum Interpolation Sea Surface Temperature (DOISST)
728 Version 2.1. *Journal of Climate*, 34(8), 2923–2939. [https://doi.org/10.1175/JCLI-D-20-](https://doi.org/10.1175/JCLI-D-20-0166.1)
729 0166.1

730 Hughs, E., & Jeantet, D. (2023, November 15). It’s not yet summer in Brazil, but a dangerous
731 heat wave is sweeping the country. Retrieved May 14, 2024, from
732 [https://apnews.com/article/brazil-heat-wave-climate-environment-wildfires-](https://apnews.com/article/brazil-heat-wave-climate-environment-wildfires-1e4714fb2c6566120c13cf4e2b657f7d)
733 1e4714fb2c6566120c13cf4e2b657f7d

734 Instituto Brasileiro de Geografia e Estatística. (2022). Demographic Census 2022. Retrieved
735 from [https://sidra.ibge.gov.br/pesquisa/censo-demografico/demografico-2022/primeiros-](https://sidra.ibge.gov.br/pesquisa/censo-demografico/demografico-2022/primeiros-resultados-populacao-e-domicilios)
736 resultados-populacao-e-domicilios

737 Ivanovich, C. C., Horton, R. M., Sobel, A. H., & Singh, D. (2024). Subseasonal Variability of
738 Humid Heat During the South Asian Summer Monsoon. *Geophysical Research Letters*,
739 51(6), e2023GL107382. <https://doi.org/10.1029/2023GL107382>

740 Jones, C., & Carvalho, L. M. V. (2013). Climate change in the South American Monsoon
741 System: Present climate and CMIP5 projections. *Journal of Climate*, 26(17), 6660–6678.
742 <https://doi.org/10.1175/JCLI-D-12-00412.1>

743 *Jornal Nacional*. (2023, November 18). Taylor Swift: segundo show é adiado, por causa do calor
744 extremo no Rio. Retrieved April 16, 2024, from [https://g1.globo.com/jornal-](https://g1.globo.com/jornal-nacional/noticia/2023/11/18/taylor-swift-show-e-adiado-apos-morte-de-fa.ghtml)
745 nacional/noticia/2023/11/18/taylor-swift-show-e-adiado-apos-morte-de-fa.ghtml

746 Krüger, E., Gobo, J. P. A., Tejas, G. T., da Silva de Souza, R. M., Neto, J. B. F., Pereira, G., et
747 al., (2024). The impact of urbanization on heat stress in Brazil: A multi-city study. *Urban*
748 *Climate*, 53, 101827. <https://doi.org/10.1016/j.uclim.2024.101827>

749 Lanzante, J. R., Dixon, K. W., Nath, M. J., Whitlock, C. E., & Adams-Smith, D. (2018). Some
750 Pitfalls in Statistical Downscaling of Future Climate. *Bulletin of the American*
751 *Meteorological Society*, 99(4), 791–803. <https://doi.org/10.1175/BAMS-D-17-0046.1>

752 Latinović, D., Chou, S. C., Rančić, M., Medeiros, G. S., & Lyra, A. D. A. (2019).
753 Seasonal climate and the onset of the rainy season in western-central Brazil simulated by
754 Global Eta Framework model. *International Journal of Climatology*, 39(3), 1429–1445.
755 <https://doi.org/10.1002/joc.5892>

756 Lemus-Canovas, M., Insua-Costa, D., Trigo, R. M., & Miralles, D. G. (2024). Record-shattering
757 2023 Spring heatwave in western Mediterranean amplified by long-term drought. *Npj*
758 *Climate and Atmospheric Science*, 7(1), 1–8. [https://doi.org/10.1038/s41612-024-00569-](https://doi.org/10.1038/s41612-024-00569-6)
759 6

760 Libonati, R., Geirinhas, J. L., Silva, P. S., Monteiro Dos Santos, D., Rodrigues, J. A., Russo, A.,
761 et al., (2022). Drought–heatwave nexus in Brazil and related impacts on health and fires:
762 A comprehensive review. *Annals of the New York Academy of Sciences*, 1517(1), 44–
763 62. <https://doi.org/10.1111/nyas.14887>

764 Liebmann, B., & Mechoso, C. R. (2011). THE SOUTH AMERICAN MONSOON SYSTEM. In
765 C.-P. Chang, Y. Ding, N.-C. Lau, R. H. Johnson, B. Wang, & T. Yasunari, *World*
766 *Scientific Series on Asia-Pacific Weather and Climate* (2nd ed., Vol. 5, pp. 137–157).
767 WORLD SCIENTIFIC. https://doi.org/10.1142/9789814343411_0009

768 Lyra, G. B., Correia, T. P., de Oliveira-Júnior, J. F., & Zeri, M. (2018). Evaluation of methods of
769 spatial interpolation for monthly rainfall data over the state of Rio de Janeiro, Brazil.
770 *Theoretical and Applied Climatology*, 134(3), 955–965. [https://doi.org/10.1007/s00704-](https://doi.org/10.1007/s00704-017-2322-3)
771 017-2322-3

772 Marengo, J. A., Costa, M. C., Cunha, A. P., Espinoza, J.-C., Jimenez, J. C., Libonati, R., et al.
773 (2025). Climatological patterns of heatwaves during winter and spring 2023 and trends
774 for the period 1979–2023 in central South America. *Frontiers in Climate*, 7.
775 <https://doi.org/10.3389/fclim.2025.1529082>

776 Marengo, J. A., Liebmann, B., Grimm, A. M., Misra, V., Silva Dias, P. L., Cavalcanti, I. F. A., et
777 al., (2012). Recent developments on the South American monsoon system. *International*
778 *Journal of Climatology*, 32(1), 1–21. <https://doi.org/10.1002/joc.2254>

779 Marengo, Jose A., Soares, W. R., Saulo, C., & Nicolini, M. (2004). Climatology of the Low-
780 Level Jet East of the Andes as Derived from the NCEP–NCAR Reanalyses:
781 Characteristics and Temporal Variability. *Journal of Climate*, 17(12), 2261–2280.
782 [https://doi.org/10.1175/1520-0442\(2004\)017<2261:COTLJE>2.0.CO;2](https://doi.org/10.1175/1520-0442(2004)017<2261:COTLJE>2.0.CO;2)

783 Montini, T. L., Jones, C., & Carvalho, L. M. V. (2019). The South American Low-Level Jet: A
784 New Climatology, Variability, and Changes. *Journal of Geophysical Research:*
785 *Atmospheres*, 124(3), 1200–1218. <https://doi.org/10.1029/2018JD029634>

786 Mora, C., Dousset, B., Caldwell, I. R., Powell, F. E., Geronimo, R. C., Bielecki, C. R., et
787 al., (2017). Global risk of deadly heat. *Nature Climate Change*, 7(7), 501–506.
788 <https://doi.org/10.1038/nclimate3322>

789 Nahlik, M. J., Chester, M. V., Pincetl, S. S., Eisenman, D., Sivaraman, D., & English, P. (2017).
790 Building Thermal Performance, Extreme Heat, and Climate Change. *Journal of*
791 *Infrastructure Systems*, 23(3), 04016043. [https://doi.org/10.1061/\(asce\)is.1943-](https://doi.org/10.1061/(asce)is.1943-555x.0000349)
792 [555x.0000349](https://doi.org/10.1061/(asce)is.1943-555x.0000349)

793 NASA JPL. (2024, January 23). El Niño 2023 | El Niño/La Niña Watch & PDO. Retrieved May
794 14, 2024, from [https://sealevel.jpl.nasa.gov/data/el-nino-la-nina-watch-and-pdo/el-nino-](https://sealevel.jpl.nasa.gov/data/el-nino-la-nina-watch-and-pdo/el-nino-2023)
795 [2023](https://sealevel.jpl.nasa.gov/data/el-nino-la-nina-watch-and-pdo/el-nino-2023)

796 Nguyen, B. (2023, December 27). Brazilian Taylor Swift Fan Died Of Heat Exhaustion At Rio
797 Concert. Retrieved April 16, 2024, from
798 [https://www.forbes.com/sites/britneynguyen/2023/12/27/brazilian-taylor-swift-fan-died-](https://www.forbes.com/sites/britneynguyen/2023/12/27/brazilian-taylor-swift-fan-died-of-heat-exhaustion-at-rio-concert/)
799 [of-heat-exhaustion-at-rio-concert/](https://www.forbes.com/sites/britneynguyen/2023/12/27/brazilian-taylor-swift-fan-died-of-heat-exhaustion-at-rio-concert/)

800 Palma, E. D., & Matano, R. P. (2009). Disentangling the upwelling mechanisms of the South
801 Brazil Bight. *Continental Shelf Research*, 29(11), 1525–1534.
802 <https://doi.org/10.1016/j.csr.2009.04.002>

803 Pampuch, L. A., Bueno, P. G., Reboita, M. S., Tomaziello, A. C. N., Nunes, A. M. P., Cardoso,
804 A. A., et al. (2025). Brazil climate highlights 2023. *Annals of the New York Academy of*
805 *Sciences*, 1549(1), 120–138. <https://doi.org/10.1111/nyas.15394>

806 Pascale, S., Carvalho, L. M. V., Adams, D. K., Castro, C. L., & Cavalcanti, I. F. A. (2019).
807 Current and Future Variations of the Monsoons of the Americas in a Warming Climate.
808 *Current Climate Change Reports*, 5(3), 125–144. [https://doi.org/10.1007/s40641-019-](https://doi.org/10.1007/s40641-019-00135-w)
809 [00135-w](https://doi.org/10.1007/s40641-019-00135-w)

810 Pepin, N., Bradley, R. S., Diaz, H. F., Baraer, M., Caceres, E. B., Forsythe, N., et al., (2015).
811 Elevation-dependent warming in mountain regions of the world. *Nature Climate Change*,
812 5(5), 424–430. <https://doi.org/10.1038/nclimate2563>

813 Périard, J. D., Racinais, S., & Sawka, M. N. (2015). Adaptations and mechanisms of human heat
814 acclimation: Applications for competitive athletes and sports. *Scandinavian Journal of*
815 *Medicine & Science in Sports*, 25 Suppl 1, 20–38. <https://doi.org/10.1111/sms.12408>

816 Powis, C. M., Byrne, D., Zobel, Z., Gassert, K. N., Lute, A. C., & Schwalm, C. R. (2023).
817 Observational and model evidence together support wide-spread exposure to
818 noncompensable heat under continued global warming. *Science Advances*, 9(36),
819 eadg9297. <https://doi.org/10.1126/sciadv.adg9297>

820 Perkins-Kirkpatrick, S., Barriopedro, D., Jha, R., Wang, L., Mondal, A., Libonati, R., &
821 Kornhuber, K. (2024). Extreme terrestrial heat in 2023. *Nature Reviews Earth &*
822 *Environment*, 5(4), 244–246. <https://doi.org/10.1038/s43017-024-00536-y>

823 Perkins, S. E., Pitman, A. J., Holbrook, N. J., & McAneney, J. (2007). Evaluation of the AR4
824 Climate Models' Simulated Daily Maximum Temperature, Minimum Temperature, and
825 Precipitation over Australia Using Probability Density Functions. *Journal of Climate*,
826 20(17), 4356–4376. <https://doi.org/10.1175/JCLI4253.1>

827 Raia, A., & Cavalcanti, I. F. A. (2008). The Life Cycle of the South American Monsoon System.
828 *Journal of Climate*, 21(23), 6227–6246. <https://doi.org/10.1175/2008JCLI2249.1>

829 Raymond, C., & Mankin, J. S. (2019). Assessing present and future coastal moderation of
830 extreme heat in the Eastern United States. *Environmental Research Letters*, 14(11),
831 114002. <https://doi.org/10.1088/1748-9326/ab495d>

832 Raymond, C., Matthews, T., & Horton, R. M. (2020). The emergence of heat and humidity too
833 severe for human tolerance. *Science Advances*, 6(19), eaaw1838.
834 <https://doi.org/10.1126/sciadv.aaw1838>

835 Raymond, C., Waliser, D., Guan, B., Lee, H., Loikith, P., Massoud, E., et al., (2022). Regional
836 and Elevational Patterns of Extreme Heat Stress Change in the US. *Environmental*
837 *Research Letters*. <https://doi.org/10.1088/1748-9326/ac7343>

838 Regoto, P., Dereczynski, C., Chou, S. C., & Bazzanella, A. C. (2021). Observed changes in air
839 temperature and precipitation extremes over Brazil. *International Journal of Climatology*,
840 41(11), 5125–5142. <https://doi.org/10.1002/joc.7119>

841 Rehbein, A., & Ambrizzi, T. (2023). ENSO teleconnections pathways in South America. *Climate*
842 *Dynamics*, 61(3), 1277–1292. <https://doi.org/10.1007/s00382-022-06624-3>

843 Ritchie, J., & Dowlatabadi, H. (2017). Why do climate change scenarios return to coal? *Energy*,
844 140, 1276–1291. <https://doi.org/10.1016/j.energy.2017.08.083>

845 Rogero, T. (2024, May 19). Brazil counts cost of worst-ever floods with little hope of waters
846 receding soon. *The Guardian*. Retrieved from
847 <https://www.theguardian.com/world/article/2024/may/19/brazil-floods-toll>

848 Rogers, C. D. W., Ting, M., Li, C., Kornhuber, K., Coffel, E. D., Horton, R. M., et al., (2021).
849 Recent Increases in Exposure to Extreme Humid-Heat Events Disproportionately Affect
850 Populated Regions. *Geophysical Research Letters*, 48(19).
851 <https://doi.org/10.1029/2021GL094183>

852 Shimizu, M. H., & Ambrizzi, T. (2016). MJO influence on ENSO effects in precipitation and
853 temperature over South America. *Theoretical and Applied Climatology*, 124(1), 291–301.
854 <https://doi.org/10.1007/s00704-015-1421-2>

855 Shreevastava, A., Raymond, C., & Hulley, G. C. (2023). Contrasting Intraurban Signatures of
856 Humid and Dry Heatwaves over Southern California. *Journal of Applied Meteorology*
857 *and Climatology*, 62(6), 709–720. <https://doi.org/10.1175/JAMC-D-22-0149.1>

858 Sistema Alerta Rio da Prefeitura do Rio de Janeiro. (2024). Meteorological Data. Retrieved from
859 <https://alertario.rio.rj.gov.br/download/dados-meteorologicos/>

860 Sistema IBGE de Recuperação Automática - SIDRA. (n.d.). Retrieved April 21, 2024, from
861 <https://sidra.ibge.gov.br/pesquisa/censo-demografico/demografico-2022/primeiros->
862 [resultados-populacao-e-domicilios](https://sidra.ibge.gov.br/pesquisa/censo-demografico/demografico-2022/primeiros-resultados-populacao-e-domicilios)

863 Son, J.-Y., Gouveia, N., Bravo, M. A., de Freitas, C. U., & Bell, M. L. (2016). The impact of
864 temperature on mortality in a subtropical city: effects of cold, heat, and heat waves in São
865 Paulo, Brazil. *International Journal of Biometeorology*, 60(1), 113–121.
866 <https://doi.org/10.1007/s00484-015-1009-7>

867 Stefanello, M., Ewerling da Rosa, C., Bresciani, C., Cordero Simões dos Reis, N., Stefanello
868 Facco, D., Teleginski Ferraz, S. E., et al., (2022). Spatial–temporal analysis of a summer
869 heat wave associated with downslope flows in southern Brazil: implications in the
870 atmospheric boundary layer. *Atmosphere* 14(1). 64.
871 <https://doi.org/10.3390/atmos14010064>

872 Swann, A. L. S., Longo, M., Knox, R. G., Lee, E., & Moorcroft, P. R. (2015). Future
873 deforestation in the Amazon and consequences for South American climate. *Agricultural*
874 *and Forest Meteorology*, 214–215, 12–24.
875 <https://doi.org/10.1016/j.agrformet.2015.07.006>

876 Tan, J., Zheng, Y., Tang, X., Guo, C., Li, L., Song, G., et al., (2010). The urban heat island and
877 its impact on heat waves and human health in Shanghai. *International Journal of*
878 *Biometeorology*, 54(1), 75–84. <https://doi.org/10.1007/s00484-009-0256-x>

879 Thrasher, B., Wang, W., Michaelis, A., Melton, F., Lee, T., & Nemani, R. (2022). NASA Global
880 Daily Downscaled Projections, CMIP6. *Scientific Data*, 9(1), 262.
881 <https://doi.org/10.1038/s41597-022-01393-4>

882 United Nations Department of Economic and Social Affairs Population Division. (2022).
883 Population of Urban Agglomerations with 300,000 Inhabitants or More in 2018, by
884 country, 1950-2035 (thousands). Retrieved from
885 <https://population.un.org/wup/Download/>

886 US EPA, O. (2021, February 4). Climate Change Indicators: Heat Waves [Reports and
887 Assessments]. Retrieved April 23, 2024, from [https://www.epa.gov/climate-](https://www.epa.gov/climate-indicators/climate-change-indicators-heat-waves)
888 [indicators/climate-change-indicators-heat-waves](https://www.epa.gov/climate-indicators/climate-change-indicators-heat-waves)

889 Vecellio, D. J., Wolf, S. T., Cottle, R. M., & Kenney, W. L. (2022). Evaluating the 35°C wet-
890 bulb temperature adaptability threshold for young, healthy subjects (PSU HEAT Project).
891 *Journal of Applied Physiology*, 132(2), 340–345.
892 <https://doi.org/10.1152/jappphysiol.00738.2021>

893 Vera, C., Baez, J., Douglas, M., Emmanuel, C. B., Marengo, J., Meitin, J., et al., (2006). The
894 South American Low-Level Jet Experiment. *Bulletin of the American Meteorological*
895 *Society*, 87(1), 63–78. <https://doi.org/10.1175/BAMS-87-1-63>

896 Wilby, R. L., Kasei, R., Gough, K. V., Amankwaa, E. F., Abarike, M., Anderson, N. J., et al.,
897 (2021). Monitoring and moderating extreme indoor temperatures in low-income urban
898 communities. *Environmental Research Letters*, 16(2), 024033.
899 <https://doi.org/10.1088/1748-9326/abdbf2>

900 You, Y., Ting, M., & Biasutti, M. (2024). Climate warming contributes to the record-shattering
901 2022 Pakistan rainfall. *Npj Climate and Atmospheric Science*, 7(1), 1–8.
902 <https://doi.org/10.1038/s41612-024-00630-4>

903 Zhao, Q., Li, S., Coelho, M. S. Z. S., Saldiva, P. H. N., Hu, K., Huxley, R. R., et al., (2019). The
904 association between heatwaves and risk of hospitalization in Brazil: A nationwide time
905 series study between 2000 and 2015. PLOS Medicine, 16(2), e1002753.
906 <https://doi.org/10.1371/journal.pmed.1002753>